

**Military Technical College
Kobry El-Kobbah,
Cairo, Egypt.**



**18th International Conference
on Applied Mechanics and
Mechanical Engineering.**

EXPERIMENTAL VERIFICATION OF COMPOSITE MATERIAL WITH CHOPPED FIBER GLASS IN PHENOL AS A ROCKET NOZZLE INSULATION

A. Seif¹, H. Kamal², Kh. Shoukry², O. Kamal² and A. N. Zayed³

ABSTRACT

This work deals with the characterization of chopped fiber glass composite. The resin matrix was a phenol base. Sheets of this composite have been cured and cut to make sample specimens for testing. Four mechanical testing have been conducted for these material including tensile test at different temperatures, bending test, compression test and hardness test. Three thermal tests including thermal conductivity determination, thermal expansion coefficient determination and ablation test have been conducted. The results show that this material has very good thermal properties capable of resisting high temperatures.

A nozzle for rocket motor has been made from this material as insulators, and static firing test has been conducted and the temperatures inside this composite material have been measured. Investigation of the thermal loads response of composite nozzle has been done using FE using ANSYS package software and the calculated temperatures have been recorded from the same places that chosen in the real firing test. By comparing the measured and obtained temperature for the fiber glass, there is a great agreement between them. The selected composite material resists the high temperatures so this used as thermal protective material.

KEYWORDS

Composite, chopped fiber, mechanical properties, tensile test, compression test, hardness

¹ Egyptian Armed Forces, Email: ahmad_safe@yahoo.com.

² Egyptian Armed Forces.

³ Prof., Faculty of Engineering, Heliopolis University, Cairo, Egypt.

INTRODUCTION

The need for cheaper materials that can perform well in adverse conditions is increasing in the society. Composite materials are materials which are finding more and more applications in the aerospace, defense, marine and transportation sectors. They are replacing conventional materials like metals and alloys in various fields

Composite materials play a major role in our live, especially in aerospace application in both commercial and military fields. From the middle of 19th century the needs of the reduction in weight, higher strength and the ability of fabrication, pushed Scientifics towards the studying, analysis, improvement and using this new materials in wide ranges

In this work fiber glass with phenol as a matrix was selected to determine its mechanical and thermal properties.

Advantages of Short Fiber

Due to the necessities of low weight and high strength materials, it is required to find out the suitable substitute with low cost. Short fibers composites are the most commonly used reinforcements.

High specific strength and low thermal conductivity are the major advantages of syntactic foams[1, 2]. This composite has significant advantages such as high specific compressive strength, high damage tolerance, thermal and electrical insulation [3] and excellent damping properties [4]. One of the major advantages is its efficiency as a buoyancy material, which becomes a natural choice for insulating subsea equipment [3].

The mechanical properties of short fiber studied by Bruce F. Blumentritt et al. [5] showed that the modulus of the composite is proportional to the fiber concentration and modulus of the fiber. George C. Jacob et al. [6] studied the effect of fiber length on the energy absorption of the carbon fiber composite, and concluded that shorter fiber lengths leads to higher specific energy absorptions. Sufyan K. Garoushi et al. conducted various studies on fiber lengths varying form 1mm-6mm, and reported that the fiber length of 5mm demonstrated good mechanical properties for the resin used [7]. These studies showed an improvement in mechanical properties with an increase in fiber volume fraction. From these studies [3-5] it is clear that the fiber length and fiber volume fraction are critical parameters in determining the properties of the composite. Zhu et al. [8] proved that the reinforcement morphology had an effect on the mechanical properties of the short fiber composites. They reinforced bone shaped short fibers instead of the normal fibers which showed a significant improvement in the yielding strength and young's modulus with an effective crack bridging.

When compared to continuous fibers reinforced composites, short fibers reinforced composites can be easily processed with affordable cost. The most important factors in the short fibers reinforcement are fiber dispersion and fiber aspect ratio. The homogeneous fiber dispersion is the most important factor to enhance the mechanical properties.

Tiesong et al [9] studied the effect of fiber content on mechanical properties and fracture behavior of short carbon fiber reinforced geopolymeric matrix composites with different volume fractions. Shao et al [10] studied the effect of length and fiber orientation distributions on tensile strength of short fiber reinforced polymers using an analytical method for predicting the tensile strength of short-fiber-reinforced polymers (SFRP). The results showed that the strength of SFRP increased rapidly with the increase of the mean fiber length at small mean fiber lengths. The inclined tensile strength of fibers has a great effect on the strength of composites. According to Zhang et al [11] experimental results show that using the short chopped basalt fiber increases bending resistances concrete.

EXPERIMENTAL WORK FOR DETERMINING THE MECHANICAL PROPERTIES

For identifying material properties, some mechanical tests were conducted. The steps conducted to achieve four mechanical test which are the tensile (at different temperatures), bending, compression and hardness of the Fiber Glass. All these tests are represented as in the following.

Preparing the Tested Samples

Chopped fiber glass Fig. 1 of length 3:5 mm has been mixed with the Phenol with percentage of 6:4 then cured under pressure and temperature [12] to obtain composite materials in the sheets shape of dimensions 300*300* ≈3 mm in the cured stage as shown in Fig. 2.

To obtain the mechanical properties of this material some tests might be done which are tensile test, three point bending, the compression test and the hardness test. According to the DIN 3039 [13], the specimens were cut to make strips with dimensions 250x25x3 mm. Tapping materials have been used at the both ends of the specimens as shown in Fig 3.

The tensile test has been done to the strip specimens shown in Fig. 3. Two problems occurred while testing which were the slipping of the specimens from the tapping material and sliding was occurred between the tapping material and the jaws.

The JANNAF (Joint Army-Navy-NASA-Air Force Propulsion Committee) specimens [14-15] with dimensions as shown in Fig. 4 were used instead of the strip specimens to avoid these problems. Sample specimens were cut according to the JANNAF standard as shown in Fig. 5.

Test Machine

The ZWICK Z050 universal test machine has been used for carrying out all the mechanical tests. This machine has remote control software which could acquire record, analyze, store and print test data with minimum manual effort. The maximum permissible test load is 10KN, and the range of crosshead speed varies from 0.0005 to 1000 mm/min with accuracy 0.004 % of the set speed. The machine is provided with temperature chamber having a range varies from -70 to +250 °c. Shore D apparatus [16] will used to measure the hardness.

Test Plane

The specimens were prepared to satisfy the mechanical tests requirements as shown in Table 1 for the tensile tests, it was done at different temperatures which were (-40 °C, 25 °C, 100 °C and 200 °C). At the normal temperature 3 specimens were prepared, at -40 °C 2 specimens were prepared and one specimen for both 100 °C and 200 °C. For the compression and three points bending tests three specimens were prepared for each test and the both tests were done at normal temperature as shown in Table 1.

Measured Data for the Mechanical Properties

The tensile test

The values of the maximum stresses at different temperatures were as shown in Fig. 6 and Table 2

At normal temperature, the maximum stress for the Fiber glass reaches 22.26 *MPa* and at -40 °C it was 20.2 *MPa* with a decreasing percentage of 9.25%. When raising the temperature to 100 °C the stress decreases to 11.66 *MPa* with a decreasing percentage of 47.5% and at 200 °C the stress decreases again to 3.56 *MPa* with a decreasing percentage of 83.9 %.

Three point bending test

For the three points bending, the results are listed in Table 3.

For the bending test of the Fiber glass, the results of the maximum stress varies from 43.4 *MPa* to 47.9 *MPa* where the strain varies from 0.42% to 0.71%

The compression test

For the compression test, the results are listed in Table 4

For the compression test of Fiber Glass, the maximum stress varies from 298.22 *MPa* to 322.6 *MPa* where the strain varies from 1.4% to 1.6%.

The Hardness test

The value of hardness of the Fiber glass is 78 Shore D which means that it is in the hard zone.

EXPERIMENTAL WORK FOR DETERMINING THE THERMAL PROPERTIES

Thermal conductivity can be measured using several different instrumental techniques. One of these is based on differential scanning calorimetry (DSC). DSC is a thermal analysis technique which measures heat flow into or out of a material as a function of temperature or time. DSC is primarily used to measure transition temperatures and associated heats of reaction in materials, particularly polymers. Measurement of glass transition temperature, melting point, percentage crystallinity, degree of cure, decomposition temperature, and oxidative stability are specific examples of some of the more common DSC measurements.

The most widely used approach for making DSC measurements is the heat flux DSC, in which the sample and reference materials (usually contained in metal pans) are placed on a thermoelectric disk inside a temperature programmed environment. Heat flow in this approach is measured using the thermal equivalent of Ohm's Law where:

$$dQ/dt = dT/R \quad (1)$$

where (Q = heat, t = time, T = temperature, R = thermal resistance of thermoelectric disk) [17, 18].

Determination of a material's thermal conductivity is important in evaluating its utility for a specific application. A variety of techniques are available to determine thermal conductivity including Modulated DSC. MDSC has the advantage of widespread availability due to its use in the study of the glass transition, melting temperature, crystallization, etc. of materials.

The thermal conductivity of the polymers is an important characteristic aiding device design. Often the desired thermal conductivity is in the range 0.7 to 3.5 (W/ m °c).

ASTM Method E1952 [19] describes the measurement of thermal conductivity by Modulated DSC. It is applicable to homogeneous, non-porous solid materials with a thermal conductivity in the limited range of 0.10 to 1.0 (W/ m °c) and a temperature range from 0 to 90 °C.

The heat capacities of a thin and thick sample are measured with Modulated DSC [20, 21]. When the thin sample is encapsulated in a pan of high thermal conductivity and subjected to a temperature modulation with long period, the sample has a uniform temperature distribution, and the measured specific heat capacity is the thermodynamic heat capacity of the sample. When the thick sample is exposed to a temperature modulation at one end, the measured apparent heat capacity is lower in comparison with the thin sample, because of the non-uniform temperature distribution across the height of the sample. The apparent heat capacity is proportional to the square root of the thermal conductivity of the sample, as shown by Eqn. (2).

$$K = (8 L C^2) / (C_p M d^2 P) \quad (2)$$

K is the observed thermal conductivity in W/(m °c), **C** is the apparent heat capacity in mJ/c, **C_p** is the specific heat capacity in J/(g c), **L** is the sample height in mm, **M** is the thick sample mass in mg, **d** is the sample diameter in mm, and **P** is the modulation period in s.

Using Eqn. (1), the thermal conductivity of a sample is derived from the heat capacity measured on a sample and some geometric and experimental factors. If the thermal conductivity of the sample is low and approaches that of the surrounding purge gas, a correction to the observed thermal conductivity is necessary to compensate for heat loss through the sample side [22].

Thermal expansion coefficient also is very important factor in determining the application of the materials. Thermo-mechanical Analysis (TMA) is used to determine this coefficient.

For the thermal properties determination, a thermal conductivity and thermal expansion has been measured besides conducting the ablation test.

Test rig and preparation of samples

For identifying material thermal properties for the fiber glass / phenol, the steps conducted to achieve the thermal conductivity and thermal expansion are shown in the following.

Preparing the composite material samples

To obtain the thermal properties of these materials some tests might be done which are thermal conductivity measurement and determination of thermal expansion coefficient. Samples of diameters 5 mm was prepared to use with the DSC Q2000 apparatus to determine the thermal conductivity as shown in Fig. 7 and samples of 8*8 mm is prepared to use with the TMA apparatus to determine thermal expansion coefficient as shown in Fig. 8.

Test Machine

Differential Scanning Calorimetry (DSC) Q2000

The Differential Scanning Calorimeter (DSC) determines the temperature and heat flow associated with material transitions as a function of time and temperature. It also provides quantitative and qualitative data on endothermic (heat absorption) and exothermic (heat evolution) processes of materials during physical transitions that are caused by phase changes, melting, oxidation, and other heat-related changes. This information helps the scientist or engineer identify processing and end-use performance.

Differential scanning calorimetry (DSC) is a TA technique in which the difference in the amount of heat required to increase the temperature of a sample and reference are measured as a function of temperature.

In this technique both tested sample and reference one are maintained at nearly the same temperature throughout the experiment. The sample holder temperature increases linearly as a function of time. The reference sample should have a well-defined heat capacity over the range of temperature to be scanned. The basic principle underlying this technique is that, when the sample undergoes a physical transformation such as phase transition, more (or less) heat will need flow to it than the reference to maintain both at the same temperature. Whether more or less heat must flow to the sample depends on whether the process is exothermic or endothermic.

The DSC instrument works in conjunction with a controller and associated software to make up a thermal analysis system.

Thermo-mechanical Analysis TMA Q400

Thermo-mechanical Analysis remains one of the most basic tools of material science. The basis of TMA is the change in the dimensions of a sample as a function of temperature (TMA).

Test method

For the DSC the Conventional MDSC method is used with time period of 20 seconds and the temperature started from 0 °C to 300 °C. For the TMA the ramp method is used and temperature started from 25 °C to 800 °C.

Measured Data for DSC

The calculated thermal conductivity for the fiber glass / phenol was 0.1846 (w/m °C) and the measured specific heat for this material is shown in Fig. 9.

Measured Data for CTE

For the measured thermal expansion coefficient for the fiber glass / phenol it was -146.6 ($\mu\text{m}/\text{m}^\circ\text{C}$) while Fig. 10 shows the curves of these tests. It was expected that the results will be in a negative values for the phenolic based matrix composites [22, 23].

For the materials cured with the phenol the CTE values are negative as expected and published before, but when tracing the behavior of the composites we notice that the material (fiber) tends to expands while the phenol tends to retract at the range of temperature up to 300-400 °C, after that the matrix (phenol) overcome the fiber and retract to a lower limits.

Ablation Test

In spacecraft design, ablation is used to both cool and protect mechanical parts and/or payloads that would otherwise be damaged by extremely high temperatures. Two principal applications are heat shields for spacecraft entering a planetary atmosphere from space and cooling of rocket engine nozzles.

In a basic sense, ablative material is designed to slowly burn away in a controlled manner, so that heat can be carried away from the spacecraft by the gases generated by the ablative process while the remaining solid material insulates the craft from superheated gases. There is an entire branch of spaceflight research involving the search for new fireproofing materials to achieve the best ablative performance.[24]

Test Rig and Preparation of Samples

A test stand plate Fig 11 has been made to carry this test. Sample of \varnothing 110 mm of the fiber glass / phenol was prepared to do this test Fig 12. Rectangular steel plate was made to carry the sample The Oxyacetylene flame was adapted to 2300 °C and the test was hold for 60 S. The weight is measured for the sample before and after the test to calculate the decrease in the materials. K type thermo-couple was placed at the rear of the steel plate connected with a data acquisition to measure the temperature during the test and continued in measuring five minutes after the test to

study the behavior of the insulation materials with the elevated temperatures as shown on Fig. 13.

Measured Data from Ablation Test

Result have been obtained from ablation test are illustrated in the following Figure 14 shows the temperature history for the Fiber glass/ phenol the measured temperature reached 73.96 °C after 81.7 second.

APPLICATIONS OF COMPOSITE MATERIALS IN NOZZLE RM

Rocketry industry is one of the strategic industries for every country. This industry is considered a measure for the country power and progress. Within the last decades, much progress has been made in this field. The rapid growth in computing speed and memory capacity of digital computers reduced the cost and time of design and production in this industry. In addition, the progress in material science highly affects the rocketry industry.

A solid rocket motor nozzle is a carefully shaped aft portion of the thrust chamber that controls the expansion of the exhaust products so that the energy forms produced in the combustion chamber are efficiently converted to kinetic energy, thereby imparting thrust to the vehicle. Approximately 65 to 75 percent of total vehicle thrust is developed by acceleration of the chamber products to sonic velocity at the nozzle throat; remainder is developed in the nozzle expansion cone.

Description of the Work

Mechanical and thermal properties fiber glass / phenol is now known, and it is obvious that the suitable application of this material is to be insulating materials for applications with moderated temperatures.

Insulation of the rocket motors is a good example for these applications where the temperature reaches 2500: 3700 °c, so there is a need for a material which can withstand these moderated temperatures.

A 6 inches rocket motor has been selected to test these composite materials. With the aid of PRO-Engineer wildfire-4 modeling package, a metallic nozzle part shown in Fig. 15 has been created and manufactured. The glass / phenol composite has been manufactured as internal insulation of this nozzle. The insertion has been made from Graphite. The nozzle consists of the outer metallic part mentioned above, the composite material (insulator) and the graphite insert as shown in Fig 16 and the assembled nozzle shown in Fig. 17.

Manufacturing of the Nozzles

The nozzle was manufactured as shown in the following Fig. 18. Six inches rocket motor shown in Fig 19 was used in the experiments with a fixed test stand.

Preparation of the test places of measuring temperature

To measure the temperature during the static test four holes of \varnothing 2.5 mm were drilled in both entrance and exit areas, two holes are in the entrance and two holes are in the exit with an angle of 90° as shown in Fig 20 and Fig 21 as a drawing and in Fig 22 as manufactured real part. At the entrance the depth of hole is 27 mm while the hole depth at the exit is 17 mm. about 8 mm of composite is left between the end of the hole and the internal surfaces.

Firing test for Fiber Glass nozzle

A static firing test has been done for the 6 inches rocket motor with a fiber glass nozzle. The motor were disassembled after the test and the nozzle were in a good condition as shown in Fig. 23.

Using the ANSYS (FEM)

After building the nozzle model by the aids of Pro-engineer, ANSYS V14 is used to solve this problem as a transient thermal problem with all obtained thermal properties as inputs of the composite materials properties. For the graphite, it's thermal properties is as shown in Table 5 At normal and 2204 °C.

Using the symmetry option for simplifying the model to reduce the number of elements which will reduce the time of solution. Only a revolve cross section of 15° has been used including the places of the two holes used to measure the temperature during the firing test. Meshing has been applied to the model as shown in Fig. 24.

The initial temperature is set to be 22 °C and the temperature along the surface of the nozzle has been calculated by DF1 program and the calculated parameters is summarized in Table 6 this values has been used as thermal loads of the problem.

Obtained Results from ANSYS

After the solution has been completed, results has been obtained from the program for the distribution of the temperature along the nozzle during the period of the test (305 seconds) and some of these results are shown in the following Fig. 25 .The results show that from time zero to 5 seconds (firing time) the composite was capable of resist the temperature propagation which provided a safe firing.

The composite continued resisting the pressure and temperature while the temperature continued propagate until 50 seconds to reach the tip of the holes (which is 8 mm from the inner surface) with a value of only 30 °C.

The internal surface of the nozzle starts to cool so the temperature tends to propagate in reverse direction to the internal container inside the nozzle.

At the end of the test (305 seconds) the temperature reached 63 °C which provide a good insulation condition.

Verification of the Results of Fiber Glass with ANSYS

Comparing the measured temperature from the firing test at node 1 with that obtained from the ANSYS one we found that the two curves have the same profile and the two curves are completely identical until 120 seconds. While the measured temperature continues rising, the obtained temperature tends to be fixed as shown in fig 26 where the measured temperature reached about 79 °C and the obtained temperature reached about 63°C.

That is because the initial condition of the ANSYS after the firing period doesn't have neither real nor calculated values, so the program here considers that the temperature is dropped from initial values given during the firing to a room temperature, so the solution reaches the steady state in time and values less than that measured from the real test as the hot gases still exist affecting temperature to continue rising.

At node (3) Fig. 27 at the exit section, the both measured and obtained solution take the same behavior also. The temperature started to rise until it reaches its maximum value after about 30 seconds then it tends to decrease because the exit section is free to air and the cooling condition here is faster than the cooling inside the nozzle. Comparing the two curves there is a small difference in the values where the ANSYS solution reached the maximum of 51 °C in 14.75 seconds while the measured one reached its maximum of 49.6 C after 15.02 seconds. At the second 12, there is a complete identical between them to the second 30 where the ANSYS solution tends to be steady while the measured one tends to continue cooling until it reached 20 °C then the temperature raised again from the second 75 and the curve starts approaching the ANSYS solution. At the second 200 the two curves coincided again till the end of the test.

CONCLUSION

Thermal and structural analyses of solid rocket motor are necessary for nozzle design. The theoretical analyses give good estimation of the nozzle performance parameters to guide the designer to the critical areas of the design.

The JANNAF standard is more efficient for getting accurate results for the chopped composite materials.

At low temperatures, the composite materials become brittle, so this is the reason for decreasing the mechanical properties, also at high temperatures this composite material as shown in the reviewed papers loses its mechanical properties rapidly.

The fiber composite material has a very low thermal conductivity so it is used as thermal insulators.

For the thermal expansion coefficient, the phenol based composites have a very small negative value of the CTE and this is also required in using those materials as insulators.

From the ablation test, it was expected that the nozzle will withstand the firing test, preventing the metallic part from high temperatures.

A good agreement is recognized between the temperature measured by the experimental work and the temperature obtained by ANSYS. It gives a satisfied impression about the thermal capability of ANSYS. The calculated temperature was almost identical to the measured temperature from the firing test as at not 1 the two values of temperatures was consistence until the second 120 then the deference in measured temperature and obtained one was due the leakage in information about the temperature distribution inside the nozzle after the firing test.

Only 8 mm of composite material is sufficient to work as an insulating material in this nozzle.

REFERENCES

- [1] E. Woldesenbet, N. Gupta, and H. D. Jerro, "Effect of microballoon radius ratio on syntactic foam core sandwich composites," *Journal of Sandwich Structures and Materials*, vol. 7, pp. 95-111, 2005.
- [2] L. Zhang and J. Ma, "Processing and characterization of syntactic carbon foams containing hollow carbon microspheres," *Carbon*, vol. 47, pp. 1451-1456, 2009.
- [3] N. Gupta, E. Woldesenbet, and S. Sankaran, "Response of syntactic foam core sandwich structured composites to three-point bending," *Journal of Sandwich Structures and Materials*, vol. 4, pp. 249-272, 2002.
- [4] L. Watkins and E. Hershey, "Syntactic foam thermal insulation for ultra-deepwater oil and gas pipelines," in *Offshore Technology Conference*, 2001.
- [5] B. F. Blumentritt, B. T. Vu, and S. L. Cooper, "The mechanical properties of oriented discontinuous fiber-reinforced thermoplastics. I. Unidirectional fiber orientation," *Polymer Engineering & Science*, vol. 14, pp. 633-640, 1974.
- [6] G. C. Jacob, J. M. Starbuck, J. F. Fellers, and S. Simunovic, "Effect of fiber volume fraction, fiber length and fiber tow size on the energy absorption of chopped carbon fiber-polymer composites," *Polymer composites*, vol. 26, pp. 293-305, 2005.
- [7] S. K. Garoushi, L. V. Lassila, and P. K. Vallittu, "Short fiber reinforced composite: the effect of fiber length and volume fraction," *J Contemp Dent Pract*, vol. 7, pp. 10-17, 2006.
- [8] Y. T. Zhu, J. Valdez, N. Shi, M. Lovato, M. Stout, S. Zhou, et al., "Influence of reinforcement morphology on the mechanical properties of short-fiber composites," *Processing of Metals and Advanced Materials: Modeling, Design and Properties*. Edited by Li, BQ, TMS, pp. 251-259, 1998.
- [9] T. Lin, D. Jia, M. Wang, P. He, and D. Liang, "Effects of fibre content on mechanical properties and fracture behaviour of short carbon fibre reinforced geopolymer matrix composites," *Bulletin of Materials Science*, vol. 32, pp. 77-81, 2009.
- [10] S.-Y. Fu and B. Lauke, "Effects of fiber length and fiber orientation distributions on the tensile strength of short-fiber-reinforced polymers," *Composites Science and Technology*, vol. 56, pp. 1179-1190, 1996.
- [11] G. Zak, M. Haberer, C. Park, and B. Benhabib, "Estimation of average fibre length in short-fibre composites by a two-section method," *Composites science and technology*, vol. 60, pp. 1763-1772, 2000.
- [12] S. G. A. a. K.-T. Hsiao, *Manufacturing techniques for polymer matrix composites*: © Woodhead Publishing Limited, 2012.

- [13] DIN, "ISO 3039 Corrugated fiberboard -- Determination of grammage of the component papers after separation," ed, 2010.
- [14] R. Nevière, "An extension of the time–temperature superposition principle to non-linear viscoelastic solids," *International journal of solids and structures*, vol. 43, pp. 5295-5306, 2006.
- [15] R. Gujjala, S. Ojha, S. Acharya, and S. Pal, "Mechanical properties of woven jute–glass hybrid-reinforced epoxy composite," *Journal of Composite Materials*, vol. 48, pp. 3445-3455, 2014.
- [16] L. Harper, T. Turner, N. Warrior, J. Dahl, and C. Rudd, "Characterisation of random carbon fibre composites from a directed fibre preforming process: Analysis of microstructural parameters," *Composites Part A: Applied Science and Manufacturing*, vol. 37, pp. 2136-2147, 2006.
- [17] B. ISO, "7619–1: 2010 Rubber, vulcanized or thermoplastic—Determination of indentation hardness. Part 1: Durometer method (Shore hardness)," *British Standards Institution: London, UK*, 2010.
- [18] R. Blaine and S. Marcus, "Derivation of temperature-modulated DSC thermal conductivity equations," *Journal of thermal analysis and calorimetry*, vol. 54, pp. 467-476, 1998.
- [19] S. M. Marcus and R. L. Blaine, "Thermal conductivity of polymers, glasses and ceramics by modulated DSC," *Thermochimica Acta*, vol. 243, pp. 231-239, 1994.
- [20] A. International, "E 1952, "Method for Thermal Conductivity and Thermal Diffusivity by Modulated Temperature Differential Scanning Calorimetry"," ed. West Conshohocken, PA.
- [21] ASTM, "ASTM Test Method E1225 Thermal Conductivity of Solids by Means of the Guarded- comparative-Longitudinal Heat Flow Technique," ed. *Annual Book of ASTM Standards: vol. 14.02*.
- [22] E. Verdonck and G. Dreezen, "Thermal Conductivity Measurements of Conductive Epoxy Adhesives by MDSC," *Thermal Library Application Brief TA312*, TA Instruments New Castle, Delaware.
- [23] B. Rath, S. Ghanwat, S. Kaity, C. Danani, R. Kulkarni, V. Alur, et al., "Thermal Conductivity of Composites of Beryllia and Lithium Titanate," *Journal of materials engineering and performance*, vol. 22, pp. 3455-3460, 2013.
- [24] R. Luo, T. Liu, J. Li, H. Zhang, Z. Chen, and G. Tian, "Thermophysical properties of carbon/carbon composites and physical mechanism of thermal expansion and thermal conductivity," *Carbon*, vol. 42, pp. 2887-2895, 2004.
- [25] J. Parker and C. M. Hogan, "Techniques for Wind Tunnel assessment of Ablative Materials," *NASA Ames Research Center, Technical Publication*, 1965.
- [26] S. T. Peters, *Handbook of composites: Springer Science & Business Media*, 2013.
- [27] J. R. Davis, P. Allen, S. Lampman, T. B. Zorc, S. D. Henry, J. L. Daquila, et al., *Metals handbook: properties and selection: nonferrous alloys and special-purpose materials: ASM International*, 1990.



Fig. 1 Chopped Fiber glass.



Fig. 2 Fiber glass sheet.



Fig. 3 Fiber glass specimens.

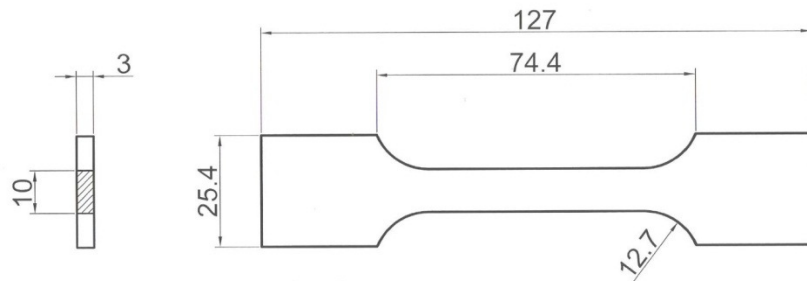


Fig. 4 Standard sample dimension with JANNAF.



Fig. 5 JANNAF samples for Fiber Glass / Epoxy.

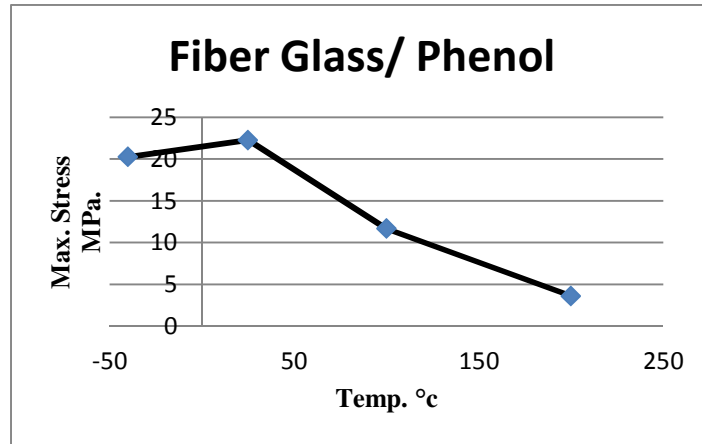


Fig. 6 Tensile strength of Fiber Glass.



Fig. 7 Samples for DSC.

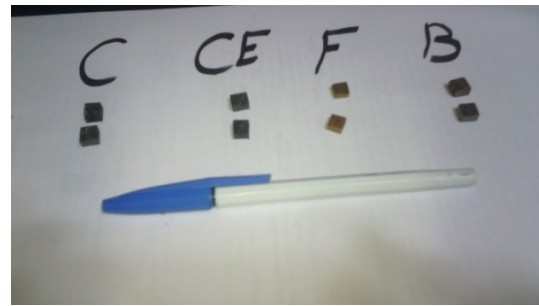


Fig. 8 Samples for TMA.

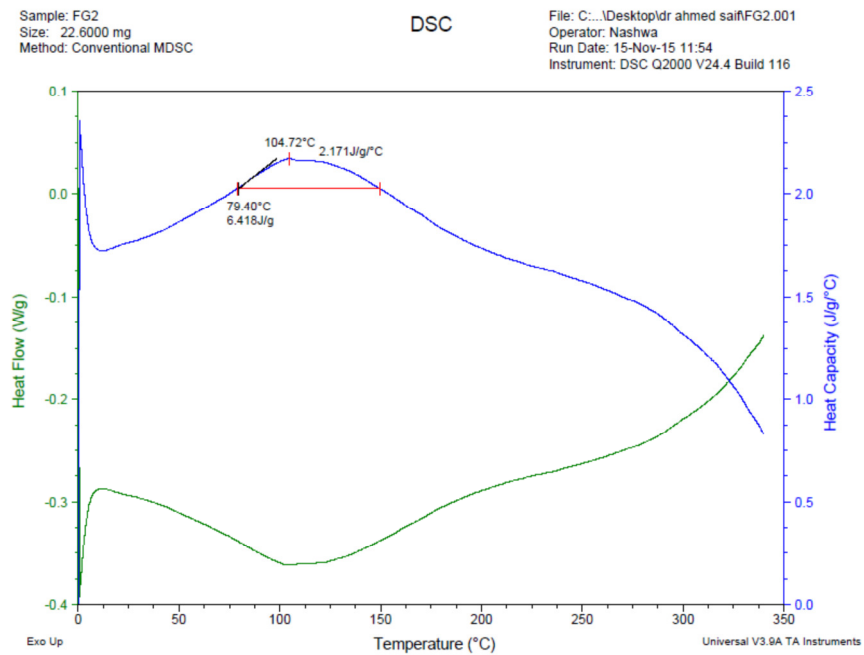


Fig. 9 Specific heat and heat capacity for the Fiber glass.

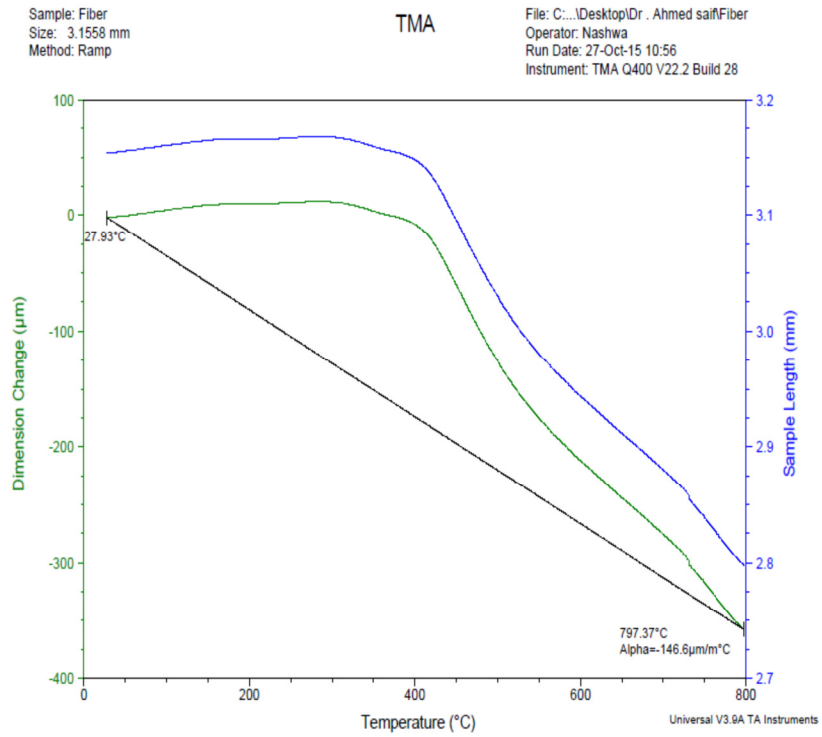


Fig. 10 CTE for Fiber glass.



Fig. 11 Test stand for ablation test.



Fig. 12 Sample for the ablation test.



a) Before the test



b) after the test

Fig. 13 Ablation test for the fiber glass/ phenol.

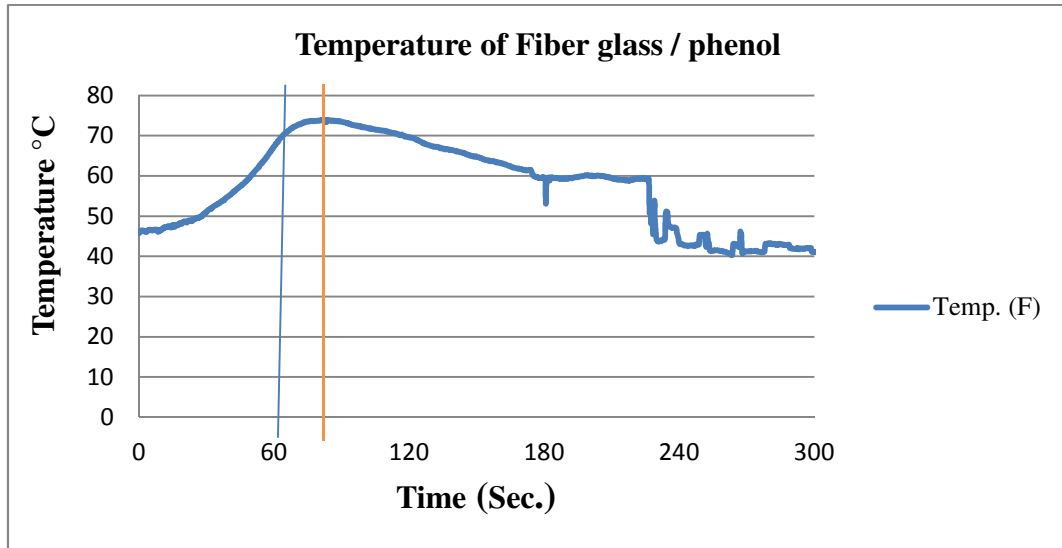


Fig. 14 Temperature history of Fiber glass / phenol.

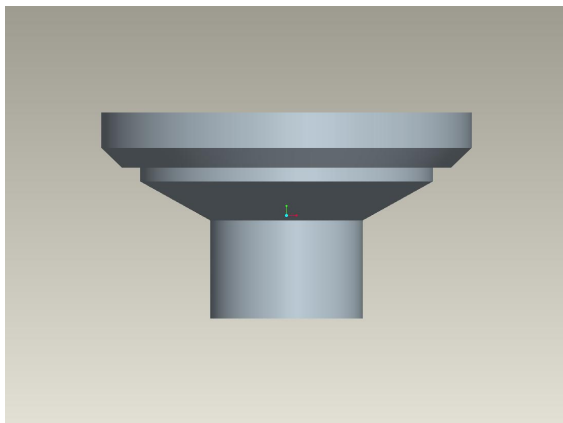


Fig. 15 Metallic nozzle part.

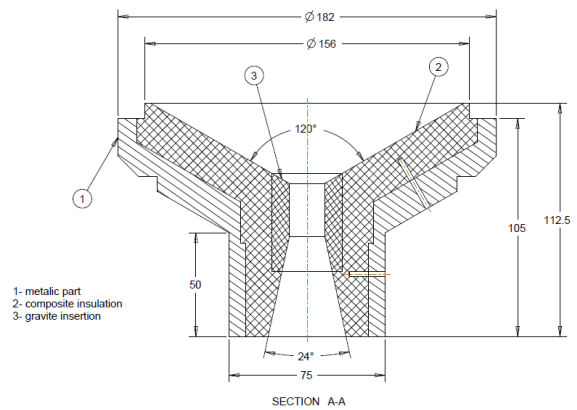


Fig. 16 Nozzle assembly and major dimension.

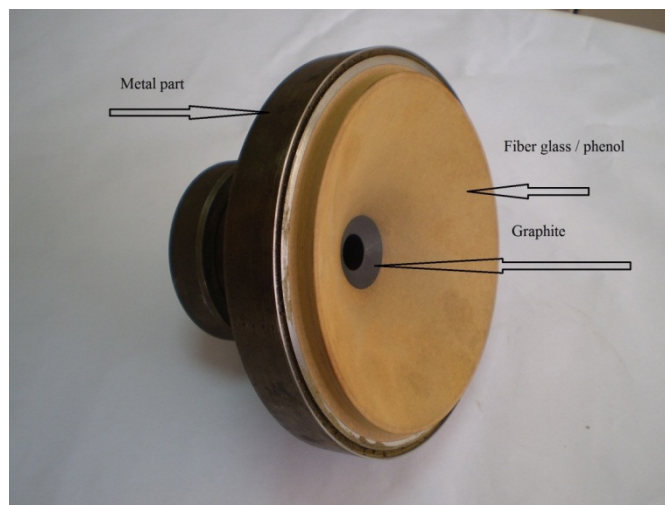


Fig. 17 Manufactured nozzle components.

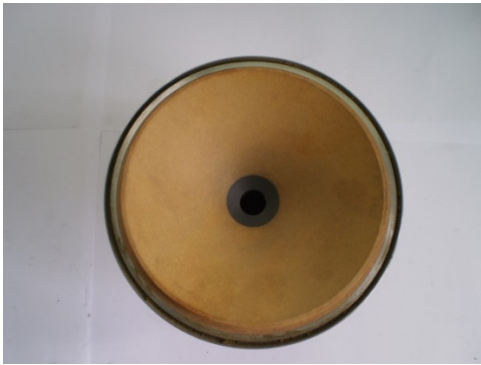


Fig. 18 Fiber Glass nozzle.



Fig. 19 Six inches rocket motor on the test stand.

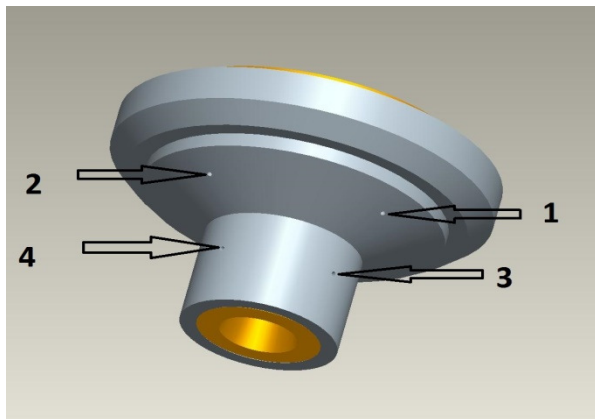


Fig. 20 Four holes places.

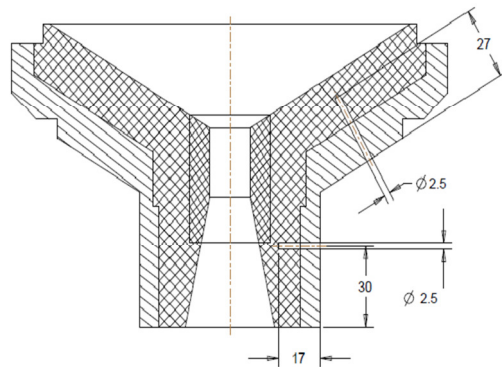


Fig. 21 Nozzle section with holes places drawing.



Fig. 22 Holes in the manufactured nozzle.



Fig. 23 Fiber Glass nozzle after the firing test.

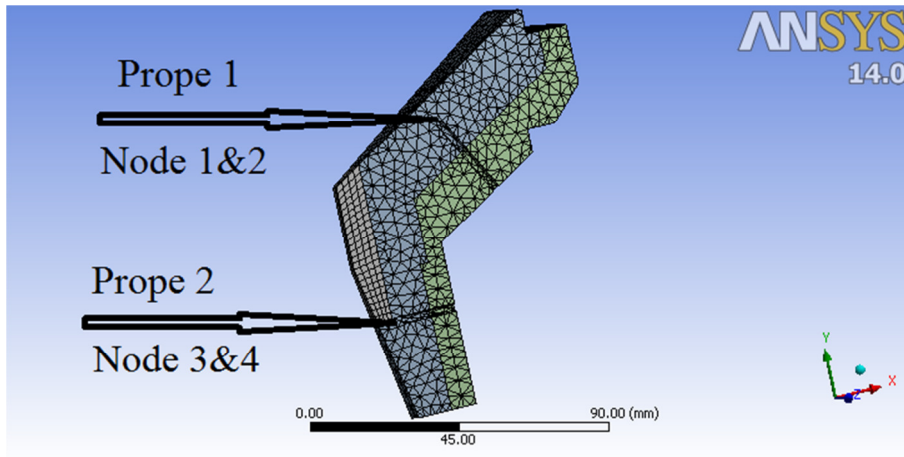


Fig. 24 Meshing of the nozzle section.

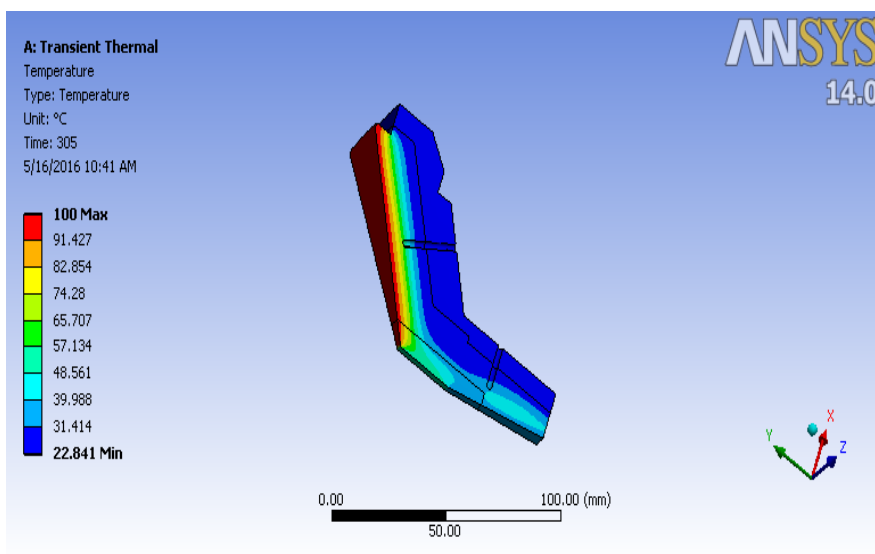


Fig. 25 Temperature result at 305 sec.

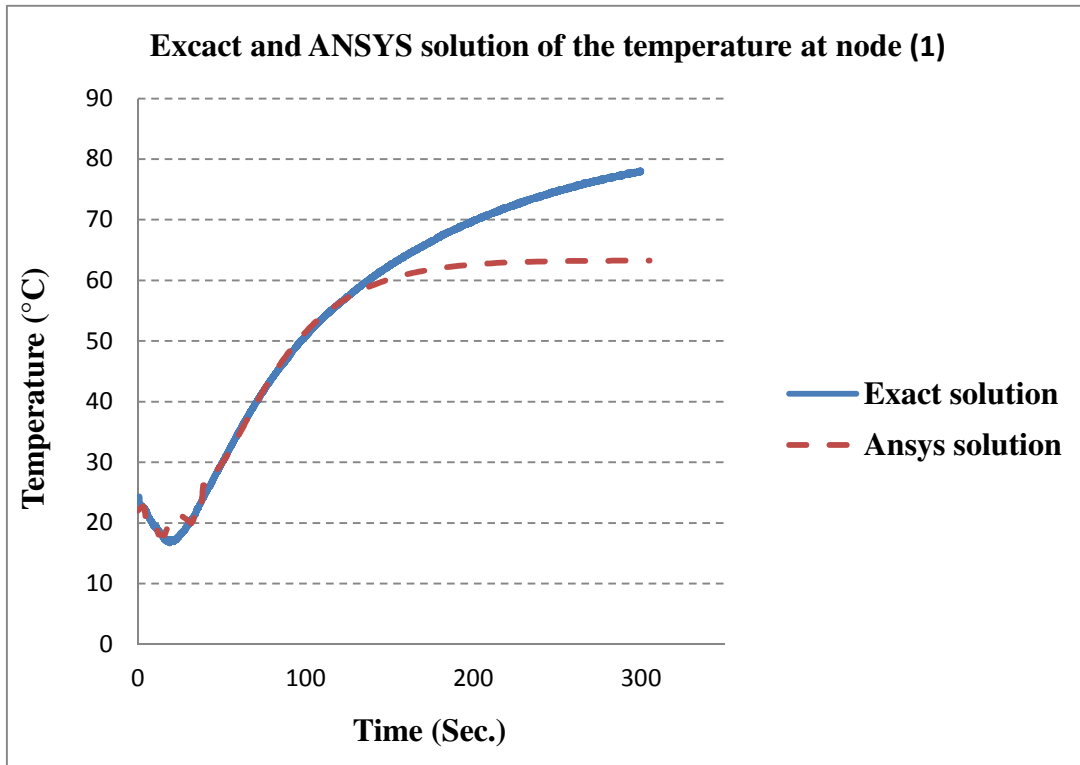


Fig. 26 Exact and ANSYS solution of the temperature at node (1).

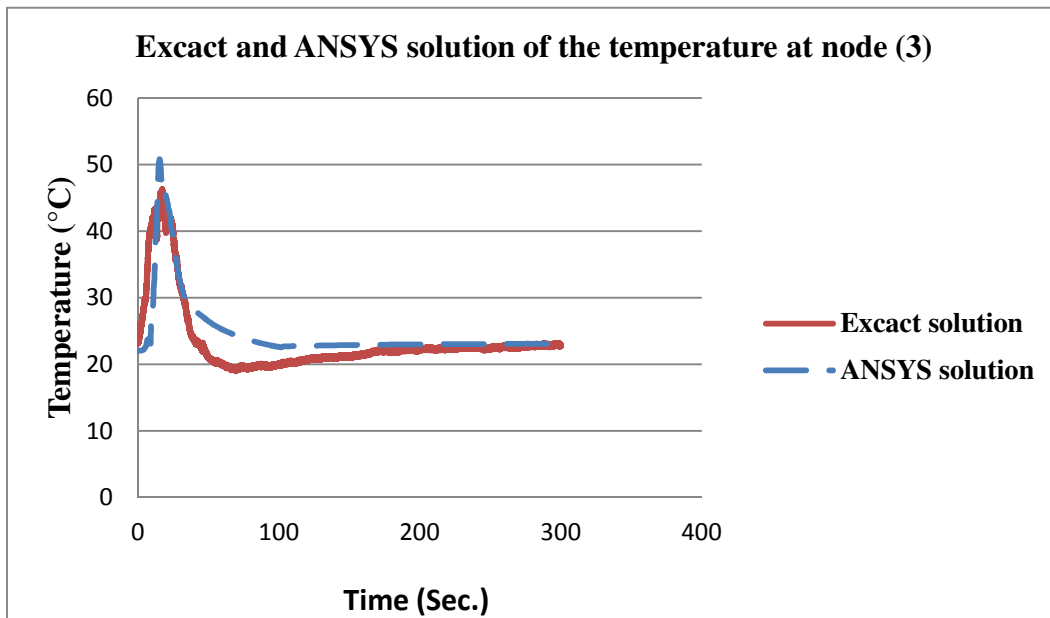


Fig. 27 Exact and ANSYS solution of the temperature at node (3).

Table 1 Test specimens' plane.

Test	Material	No. of tests at each temperature			
		-40 oC	25 oC	100 oC	200 oC
Tensile	Fiber glass/Phenol	2	3	1	1
Compression			3		
3 point Bending			3		

Table 2. Measured data for the maximum tensile strength.

Specimen No.	Temp.	Max. Stress MPa	Break Stress MPa	Max. Strain %	Strain at Break %
1	25	22.26	22.26	1.30	1.30
2		26.48	26.48	1.40	1.40
3		18.04	18.04	1.10	1.10
Average		22.26	22.26	1.26	1.26
4	-40	14.02	14.02	0.70	0.70
5		26.48	26.48	1.60	1.60
Average		20.25	20.25	1.15	1.15
6	100	11.67	11.67	1.1	1.1
7	200	3.61	3.61	0.8	0.9

Table 3 Bending test results of the Fiber Glass.

Specimen No.	Max. Stress MPa	Break Stress MPa	Max. Strain %	Strain at Break %
1	43.4	30.8	0.42	0.43
2	45.0	32.1	0.59	0.65
3	47.9	34.4	0.71	0.77
Average	45.43	32.4	0.57	0.62

Table 4 Compression test results of the Basalt.

Specimen No.	Max. Stress MPa	Break Stress MPa	Max. Strain %	Strain at Break %
1	309.89	308.90	1.5	1.5
2	298.22	297.23	1.4	1.4
3	322.6	321.65	1.6	1.6
Average	310.18	309.26	1.5	1.5

Table 5 Thermal properties of Graphite (5890) [15, 16].

Temperature °C	K [w/m. °C]	C [J/Kg. °C]	ρ [kg/m3]
20	Kx=121.1 Ky=69.20	1064	1750
2204	Kx=27.68 Ky=25.95	2510	1750

Table 6 Calculated parameters for the six inch rocket motor.

Combustion chamber pressure Pa	Exit pressure Pa	Critical section pressure Pa	Burning rate m/sec,	kapa	C*
6939050	222860	3836690	0.00665	0.6608	1551
Combustion chamber temperature °C	Exit temperature °C	Critical section temperature °C	Specific heat ratio	m° Kg/sec.	Expansion ratio
3298	1480.79	2886	1.2608	1.07647	4.59184